

# Coordination of LiH Molecules to Mo≡Mo Bonds: Experimental and Computational Studies on Mo<sub>2</sub>LiH<sub>2</sub>, Mo<sub>2</sub>Li<sub>2</sub>H<sub>4</sub>, and Mo<sub>6</sub>Li<sub>9</sub>H<sub>18</sub> Clusters

Marina Perez-Jimenez, Natalia Curado, Celia Maya, Jesus Campos, Jesus Jover, Santiago Alvarez,\* and Ernesto Carmona\*

Cite This: *J. Am. Chem. Soc.* 2021, 143, 5222–5230

Read Online

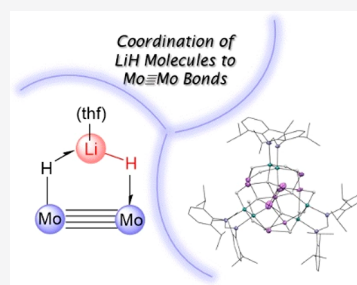
ACCESS |

Metrics & More

Article Recommendations

Supporting Information

**ABSTRACT:** The reactions of LiAlH<sub>4</sub> as the source of LiH with complexes that contain (H)Mo≡Mo and (H)Mo≡Mo(H) cores stabilized by the coordination of bulky Ad<sup>Dipp2</sup> ligands result in the respective coordination of one and two molecules of (thf)LiH, with the generation of complexes exhibiting one and two HLi(thf)H ligands extending across the Mo≡Mo bond (Ad<sup>Dipp2</sup> = HC(NDipp)<sub>2</sub>; Dipp = 2,6-*i*-Pr<sub>2</sub>C<sub>6</sub>H<sub>3</sub>; thf = tetrahydrofuran, C<sub>4</sub>H<sub>8</sub>O). A theoretical study reveals the formation of Mo–H–Li three-center–two-electron bonds, supplemented by the coordination of the Mo≡Mo bond to the Li ion. Attempts to construct a [Mo<sub>2</sub>{HLi(thf)H}<sub>3</sub>(Ad<sup>Dipp2</sup>)<sub>2</sub>] molecular architecture led to spontaneous trimerization and the formation of a chiral, hydride-rich Mo<sub>6</sub>Li<sub>9</sub>H<sub>18</sub> supramolecular organization that is robust enough to withstand the substitution of lithium-solvating molecules of tetrahydrofuran by pyridine or 4-dimethylaminopyridine.



## INTRODUCTION

Along with noble gas helium, hydrogen and lithium are the simplest, lightest elements and the only ones that existed in the young universe.<sup>1</sup> Helium hydride, HeH<sup>+</sup>, is a molecule of astrophysical importance,<sup>2</sup> whereas LiH is the lightest metal hydride and arouses considerable interest due to its many applications.<sup>3–5</sup> In the gas phase, molecules of LiH exist as a result of the overlap of the singly occupied H 1s and Li 2s atomic orbitals,<sup>6</sup> with an experimentally determined interatomic distance of *ca.* 1.60 Å.<sup>7</sup> In the solid state, LiH adopts a cubic NaCl-type structure, characterized by long Li⋯H contacts of approximately 2.04 Å.<sup>3</sup>

Molecular hydrides of the s-block elements have been intensively investigated in recent years. For group 2 metals, new, uncommon structures and a diversity of useful applications in hydrometalation, hydrogenation, and other reactions have been uncovered, thanks in no small part to the use of sterically encumbered auxiliary ligands.<sup>3,8–19</sup> Progress for the alkali metals has been more limited, although with notable exceptions. These include Stasch's hydrocarbon-soluble lithium hydride cluster [(DippNPPPh)<sub>3</sub>Li]<sub>4</sub>(LiH)<sub>4</sub>, containing a (LiH)<sub>4</sub> central cube (Dipp = 2,6-*i*-Pr<sub>2</sub>C<sub>6</sub>H<sub>3</sub>),<sup>20</sup> as well as the generation by Mulvey and co-workers of hexane-soluble lithium hydride transfer reagents.<sup>21,22</sup> Of particular relevance is the synthesis of the dilithiozincate hydride [(tmed)Li]<sub>2</sub>[(<sup>i</sup>PrNCH<sub>2</sub>CH<sub>2</sub>N(<sup>i</sup>Pr))Zn(<sup>i</sup>Bu)H] that retains the Li–H bond in solution and undergoes the dynamic association and dissociation of (tmed)LiH.<sup>21</sup> Also noteworthy are reports on hydride encapsulation by molecular alkali metal clusters,<sup>23</sup> the structural characterization of the LiH and

LiO<sup>*t*</sup>Bu agglomerate Li<sub>33</sub>H<sub>17</sub>(O<sup>*t*</sup>Bu)<sub>16</sub>,<sup>24</sup> and the synthesis of a (LiH)<sub>4</sub> cube coordinated to three bis(amido)alane units.<sup>25</sup>

Transition-metal complexes allegedly containing coordinated monomeric molecules of LiH are sparse. There are, however, some reports describing M–H–Li systems where a degree of covalent bonding within the bridging bond can be proposed on the basis of the observation of one-bond <sup>1</sup>H–<sup>6,7</sup>Li NMR coupling constants.<sup>21,26–35</sup> Despite the scarcity of complexes of this type, it is conceivable that, like other main-group metal–hydrogen bonds (e.g., Mg–H, Al–H, and Zn–H),<sup>36–44</sup> a molecule of lithium hydride might bind to a transition-metal fragment through its Li–H bond, assisted by an interaction with an adjoining ligand that could compensate for the unsaturation of the lithium coordination shell and further heighten the σ-donor strength of the polar Li–H bond.

In this context, we envisioned that quadruply bonded hydride central units [Mo<sub>2</sub>(H)<sub>*n*</sub>] (*n* = 1, 2) could be utilized to build the target molecular architectures. As represented in structure A of Figure 1, such dimolybdenum dihydride units possess strong hydride character<sup>45</sup> and feature Mo–Mo separations of close to 2.10 Å, with Mo–H vectors nearly perpendicular to the Mo–Mo bond.<sup>45</sup> Here, we discuss the

Received: February 9, 2021

Published: March 23, 2021



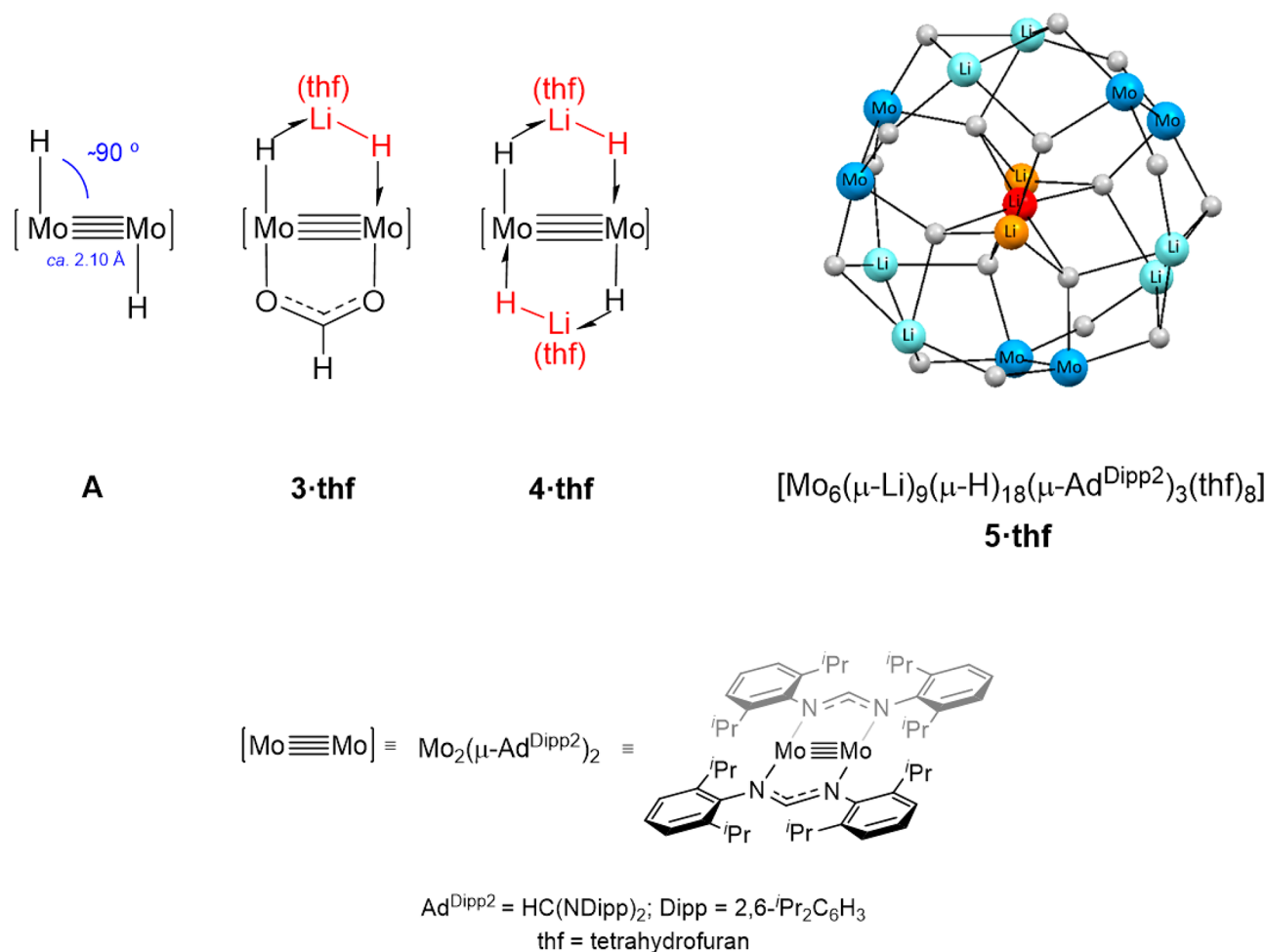


**Figure 1.** Simplified representations of the structures of complexes **3·thf**–**5·thf**. The three structural types originate from  $[\text{Mo}_2(\text{H})_n]$  cores by the incorporation of one, two, or three molecules of  $(\text{thf})\text{LiH}$  ( $n = 1$ , complex **3·thf**;  $n = 2$ , **A** and complex **4·thf**; when  $n = 3$ , the unobserved monomer trimerizes to complex **5·thf** with the loss of a molecule of tetrahydrofuran). In the structure of **5·thf**, symmetry-related lithium atoms share the same color.

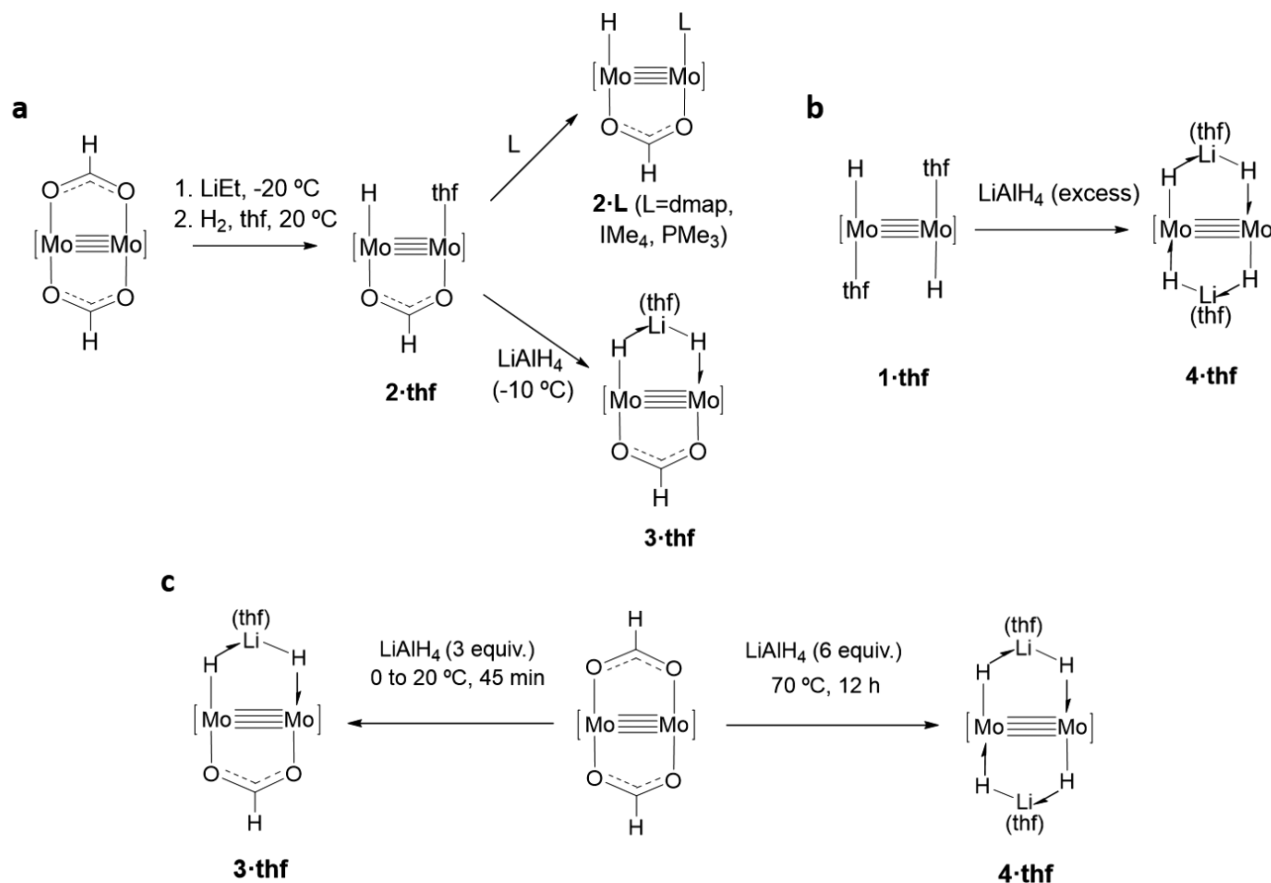
synthesis and structure of complexes **3·thf** and **4·thf** (Figure 1) that contain one and two formally monoanionic, bridging  $\text{H}-\text{Li}(\text{thf})-\text{H}$  ligands, respectively, spanning the  $\text{Mo}\equiv\text{Mo}$  bond. We also study the unexpected formation of a unique, hydrocarbon-soluble, hydride-rich  $\text{Mo}_6\text{Li}_9\text{H}_{18}$  cluster, **5·thf**, formally resulting from the trimerization of unobserved monomer  $[\text{Mo}_2\{\mu\text{-HLi}(\text{thf})\text{H}\}_3(\mu\text{-Ad}^{\text{Dipp}2})]$ , with the loss of a molecule of tetrahydrofuran. Throughout this article, three-center–two-electron ( $3c-2e$ ) interactions implicating  $\text{Mo}-\text{H}$  and  $\text{Li}-\text{H}$  bonds are represented with the aid of the half-arrow formalism proposed by Green, Green, and Parkin.<sup>46</sup>

## RESULTS AND DISCUSSION

In recent work, we showed that tetrahydrofuran adduct  $[\text{Mo}_2(\text{H})_2(\mu\text{-Ad}^{\text{Dipp}2})_2(\text{thf})_2]$  (**1·thf**, where  $\text{Ad}^{\text{Dipp}2} = \text{HC}(\text{NDipp})_2$  and  $\text{Dipp} = 2,6\text{-}^i\text{Pr}_2\text{C}_6\text{H}_3$ ) is a convenient source of unsaturated dihydride  $[\text{Mo}_2(\text{H})_2(\mu\text{-Ad}^{\text{Dipp}2})_2]$  containing a *trans*-( $\text{H})\text{Mo}\equiv\text{Mo}(\text{H})$  core (structure **A** in Figure 1).<sup>45</sup> The  $\text{Mo}_2(\text{H})_2$  functionality of this complex was engendered by hydrogenolysis of the  $\text{Mo}-\text{C}$  bonds of the  $[(\text{Me})\text{Mo}\equiv\text{Mo}(\text{Me})]$  homologue,<sup>47</sup> a method that continues to be a main vehicle for the synthesis of transition-metal hydrides. Searching for a related monohydride  $[(\text{H})\text{Mo}\equiv\text{Mo}]$  core, we carried out the two-step transformation shown in Scheme 1a. Low-

temperature alkylation of  $[\text{Mo}_2(\mu\text{-O}_2\text{CH})_2(\mu\text{-Ad}^{\text{Dipp}2})_2]$  with equimolar amounts of  $\text{LiEt}$  yielded an ethyl-formate intermediate that was reacted *in situ* with  $\text{H}_2$  and converted to the hydride-formate product, **2·thf** (Scheme 1), in good isolated yields (ca. 70%). The coordinated tetrahydrofuran molecule of **2·thf** is highly labile, and it was readily replaced by Lewis bases such as 4-dimethylaminopyridine (dmap), 1,3,4,5-tetramethylimidazol-2-ylidene ( $\text{IMe}_4$ ), and  $\text{PMe}_3$ , giving complexes **2·L** (Scheme 1a, top). Similarly, the use of  $\text{LiAlH}_4$  as a source of  $\text{LiH}$  permitted the isolation of complex **3·thf** that was obtained as a yellow solid in yields of around 60%. This reaction was not, however, simple and also produced related derivative **4·thf**, along with minute amounts of a tetrahydroaluminate complex to be described elsewhere. Complex **3·thf** possesses a  $\text{H}-\text{Mo}\equiv\text{Mo}-\text{H}-\text{Li}(\text{thf})$  chelate moiety resulting from the substitution of the coordinated tetrahydrofuran of **2·thf** by a molecule of  $(\text{thf})\text{LiH}$ , with the formation of a  $\sigma\text{-Li}-\text{H}$  complex, that becomes stabilized by the concomitant formation of a  $3c-2e$   $\text{Mo}-\text{H}\rightarrow\text{Li}$  bond involving the adjacent  $\text{Mo}-\text{H}$  terminus.

Next, **1·thf** was utilized as a source of the  $[\text{Mo}_2(\text{H})_2]$  center (Scheme 1b). Mixing a tetrahydrofuran solution of this complex with a solution of  $\text{LiAlH}_4$  in the same solvent caused the immediate precipitation of a bright-yellow solid that was

Scheme 1. Synthesis of Hydride Complexes with Mo≡Mo Bonds<sup>a</sup>

<sup>a</sup>(a) Compounds **2·thf**, **2·L**, and **3·thf**. (b and c) Direct synthesis of complexes **3·thf** and **4·thf**. [Mo≡Mo] is an abbreviation for Mo<sub>2</sub>(μ-Ad<sup>Dipp2</sup>)<sub>2</sub>. L is 4-dimethylaminopyridine (dmap), 1,3,4,5-tetramethylimidazol-2-ylidene (IMe<sub>4</sub>), and PMe<sub>3</sub>.

identified as dilithium tetrahydride dimolybdenum complex [Mo<sub>2</sub>{μ-HLi(thf)H}<sub>2</sub>(μ-Ad<sup>Dipp2</sup>)<sub>2</sub>] (**4·thf**), that is, as a Mo<sub>2</sub>Li<sub>2</sub>H<sub>4</sub> cluster. As drawn in Scheme 1b, the compound contains two *trans*-[μ-HLi(thf)H] ligands that extend across the Mo≡Mo bond. Thus, it can be related to **3·thf** by means of formal replacement of the bridging formate of the latter by a second μ-Li(thf)H<sub>2</sub><sup>-</sup> three-atom chelating ligand. In agreement with this rationale, complexes **3·thf** and **4·thf** were generated in high yields (70–85%) by the more direct method summarized in Scheme 1c, based on the reaction of readily available [Mo<sub>2</sub>(μ-O<sub>2</sub>CH)<sub>2</sub>(μ-Ad<sup>Dipp2</sup>)<sub>2</sub>] with LiAlH<sub>4</sub> under appropriate conditions.

Complexes **2·L**, **3·thf**, and **4·thf** were characterized with the aid of microanalytical, spectroscopic, and X-ray data and were additionally studied by computational methods. For molecules of **2·L**, the proposed structure is based on IR and NMR data and was unmistakably confirmed by X-ray crystallography for **2·IMe<sub>4</sub>** (Figure S1). Regarding complexes **3·thf** and **4·thf**, their hydride signals were not readily apparent in the IR spectra, possibly because of the Mo–H–Li bridging character, so the unambiguous identification of the three-atom HLiH chains in **3·thf** and **4·thf** owes much to the <sup>1</sup>H and <sup>7</sup>Li NMR experiments developed. Surprisingly more soluble in benzene and toluene than in tetrahydrofuran, the HLi(thf)H ligand in **3·thf** resonate at δ 4.33 (C<sub>6</sub>D<sub>6</sub>), appearing as a partially resolved multiplet due to coupling to the <sup>7</sup>Li (92.6%, *I* = 3/2) and <sup>6</sup>Li (7.4%, *I* = 1) nuclei. As can be seen in Figure 2, this signal becomes a singlet in the <sup>1</sup>H{<sup>7</sup>Li} NMR

spectrum. Moreover, the 4.33 multiplet is absent in the <sup>1</sup>H NMR spectrum of the DLiD isotopologue of **3·thf**, prepared by the reaction of [Mo<sub>2</sub>(μ-O<sub>2</sub>CH)<sub>2</sub>(μ-Ad<sup>Dipp2</sup>)<sub>2</sub>] with LiAlD<sub>4</sub>. The <sup>7</sup>Li{<sup>1</sup>H} NMR spectrum is a somewhat broad singlet at 3.6 ppm that transforms into a 1:2:1 triplet in the proton-coupled <sup>7</sup>Li NMR experiment, with a one-bond <sup>7</sup>Li–<sup>1</sup>H coupling constant of 16 Hz.

Complex **4·thf** is only scarcely soluble in common solvents such as benzene, toluene, and tetrahydrofuran, but it is just sufficiently soluble in C<sub>6</sub>H<sub>5</sub>F for NMR studies. Pertinent NMR data are also included in Figure 2. In particular, the Mo<sub>2</sub>LiH<sub>2</sub> moieties exhibit comparable <sup>1</sup>J(<sup>7</sup>Li–<sup>1</sup>H) couplings of 17 Hz. These observations categorically demonstrate the existence of HLiH entities coordinated to the Mo–Mo quadruple bond in the **3·thf** and **4·thf** molecules. Besides, they attest without a doubt to the fact that, although probably mainly Coulombic in nature (*vide infra*), the Mo–H–Li–H–Mo bonding interactions involve a considerable degree of covalency, that is, of substantial electron density shared among the molybdenum, hydrogen, and lithium valence orbitals. It is pertinent to remark that the observation of scalar coupling in lithium hydride complexes is rare, to the point that few <sup>1</sup>J(<sup>6,7</sup>Li–<sup>1</sup>H) values can be found in the literature.<sup>21,29–35</sup> Previously observed couplings range from approximately 6 to 15 Hz such that the 16 to 17 Hz values found for **3·thf** and **4·thf** are among the highest thus far reported. For the LiH molecule, a <sup>1</sup>J(<sup>7</sup>Li–<sup>1</sup>H) coupling constant of 159 Hz has been calculated.<sup>49</sup>

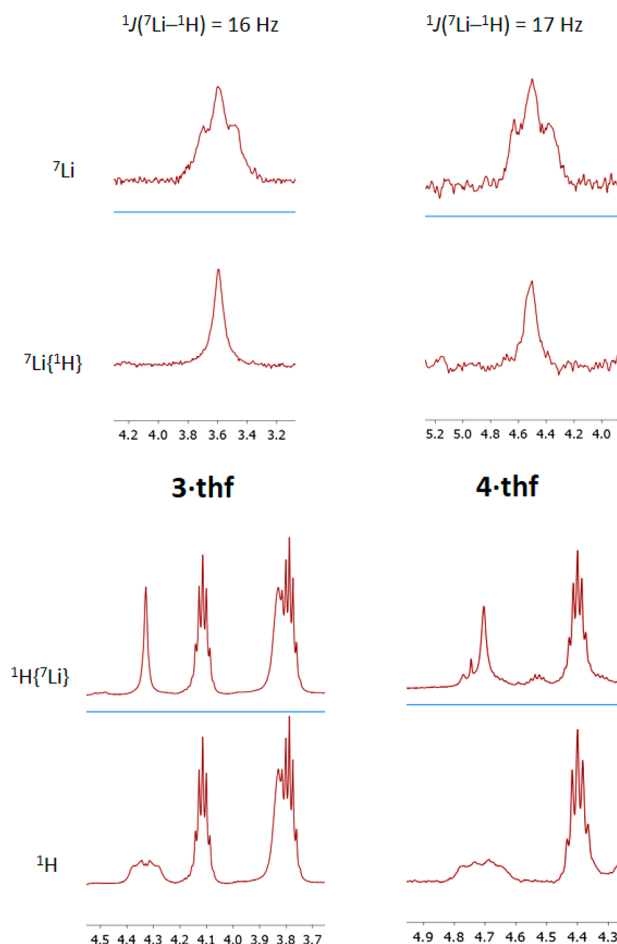


**Figure 2.** From bottom to top,  $^1\text{H}$ ,  $^1\text{H}\{^7\text{Li}\}$ ,  $^7\text{Li}\{^1\text{H}\}$ , and  $^7\text{Li}$  NMR spectra of the  $\text{HLiH}$  moieties of complexes **3•thf** (left) and **4•thf** (right).  $^1\text{H}$  resonances at lower frequency relative to  $\text{Mo}-\text{H}-\text{Li}$  are due to methine protons of the  $\text{Ad}^{\text{Dipp}2}$  ligands or to tetrahydrofuran.

Complexes **3•thf** and **4•thf** possess good thermal stability. Their  $\text{C}_6\text{D}_6$  and  $\text{C}_6\text{D}_5\text{F}$  solutions appear to be stable for 1 day at room temperature, though decomposition occurs upon heating at  $70^\circ\text{C}$  for 3 to 4 h. In the solid state, decomposition is apparent only at  $T \geq 150^\circ\text{C}$ . The two compounds behave as soluble  $\text{LiH}$  carriers, particularly **4•thf**, which is the more reactive of the two. For instance, complex **4•thf** reacted with  $\text{Ph}_2\text{C}(\text{O})$  to give the expected alkoxide  $\text{Ph}_2\text{C}(\text{H})(\text{OLi})$ .<sup>20,22</sup> Their molecular structures were investigated by X-ray crystallography and optimized by means of DFT calculations. Owing to poor crystal properties, the data collected for the former do not permit a rigorous structural discussion, particularly with respect to what concerns the geometric parameters of H atoms. Nonetheless, they allow us to define beyond any doubt the connectivity represented in Figure S2. Figure 3 contains an ORTEP representation of the molecules of **4•thf**, along with selected metrics. A more complete set of bond distances is collected in Table 1, which contains both experimental and computational data. When this manuscript was being prepared, there was no precedent for a structural motif of this kind in the Cambridge Structural Database (CSD).<sup>50</sup> The two bridging  $\text{H}-\text{Li}(\text{thf})-\text{H}$  and  $\text{Ad}^{\text{Dipp}2}$  ligands of complex **4•thf** occupy mutually trans positions, originating a typical paddle-wheel structure<sup>51–53</sup> around a  $\text{Mo}-\text{Mo}$  quadruple bond of length  $2.1006(7)$  Å. The discrepancy observed between the experimental and calculated  $\text{Mo}-\text{H}$  and

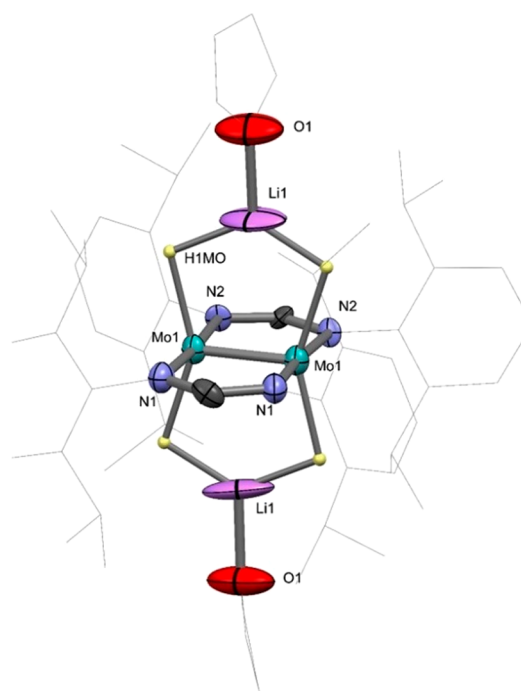


**Figure 3.** Solid-state structure of **4•thf**. Some atoms have been omitted for clarity. Thermal ellipsoids are shown at 50%. Selected bond distances (Å) and a bond angle (deg):  $\text{Mo1}-\text{Li1}$ ,  $2.91(2)$  and  $2.97(2)$ ;  $\text{Mo1}-\text{Mo1}$ ,  $2.1006(7)$ ;  $\text{Mo1}-\text{N1}$ ,  $2.10(1)$ ;  $\text{Mo1}-\text{N2}$ ,  $2.20(1)$ ;  $\text{Li1}-\text{O1}$ ,  $1.86(2)$  Å; and  $\text{N1}-\text{Mo1}-\text{Li1}$ ,  $92.1(5)$ .

**Table 1.** Selected Experimental and Computational Bond Distances (Å) for Complexes **4•thf** and **5•thf**<sup>a</sup>

|       | 4•thf |           | 5•thf                              |            |
|-------|-------|-----------|------------------------------------|------------|
|       | calcd | exp       | calcd                              | exp        |
| Mo–Mo | 2.134 | 2.1006(7) | 2.14–2.15                          | 2.10 (av.) |
| Mo–H  | 1.852 | 2.05      | 1.83–1.84 (Mo–H <sup>cent</sup> )  | 1.67–2.04  |
| Mo–Li | 2.971 | 2.97(2)   | 3.21–3.25 (Mo–Li9)                 | 3.15–3.24  |
|       | 2.968 | 2.91(2)   |                                    |            |
| Li–H  | 1.787 | 1.74      | 1.97–2.07 (Li9–H <sup>cent</sup> ) | 1.81–2.09  |
|       | 1.784 | 1.85      |                                    |            |

<sup>a</sup>For the latter complex, the  $\text{Li7/8}-\text{Li9}$  distances are 2.44 and 2.46 (calcd), 2.45 and 2.50 Å (exp), while corresponding values for the  $\text{Li7}-\text{Li9}-\text{Li8}$  angle are  $176.5$  and  $176.3^\circ$ .

$\text{Li}-\text{H}$  distances collected in Table 1 is most likely due to the uncertainty in the localization by X-ray diffraction of hydride ligands bound to a heavy atom such as molybdenum. The computed distances are 1.85 and 1.78 Å, respectively. The first is almost coincident with the average  $\text{Mo}-\text{H}-\text{Mo}$  bond lengths determined by neutron diffraction,<sup>54</sup> while the second is somewhat longer than the  $1.60$  Å value measured for the molecule of  $\text{LiH}$  in the gas phase but significantly shorter than the interatomic separation of  $2.04$  Å found for this hydride in the solid state.<sup>3</sup> Regarding the  $\text{Mo}-\text{Li}$  distances, the experimental values of  $2.91(2)$  and  $2.97(2)$  Å are indistinguishable within experimental error, whereas in the optimized structure this slight asymmetry vanishes, leading to a separation of *ca.*  $2.97$  Å. For comparison, the sum of the covalent radii of the atoms is  $2.82$  Å.<sup>55</sup>

We have carried out geometry optimization and an NBO analysis of chemical bonding within the  $\text{Mo}-\text{H}-\text{Li}-\text{H}-\text{Mo}$  rings of **4•thf**. For simplicity, we describe here the comparable



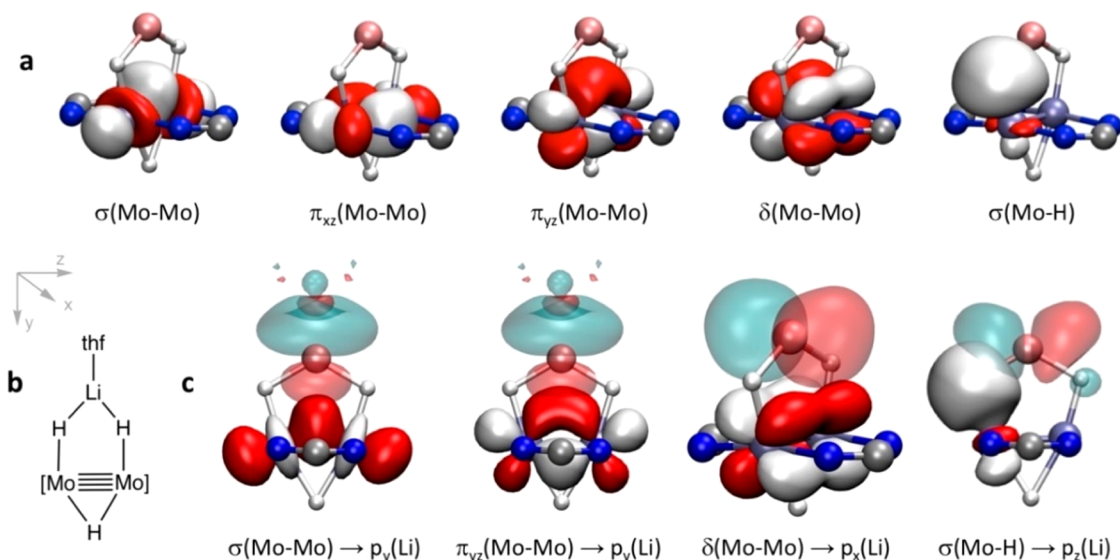


**Figure 4.** (a) Four NBO orbitals corresponding to the  $\sigma$  component, two  $\pi$  components, and one  $\delta$  component of the quadruple  $\text{Mo}\equiv\text{Mo}$  bond in  $4\cdot\text{thf}'$  and one of the  $\text{Mo}-\text{H}$   $\sigma$  bonding orbitals composed by the  $\delta(\text{Mo}-\text{Mo})$ -type  $x^2-y^2$  and the hydride  $1s$  orbitals. (b) Coordinate orientation and composition of the central fragment of the molecule shown in the orbital plots. (c) Some representative interactions between donor (white and red) and acceptor (light blue and pink) natural orbitals in  $4\cdot\text{thf}'$ .

results obtained for monolithiated species  $4\cdot\text{thf}'$ , whose structure (Figure 4b) finds precedent in that of methyl complex analog  $[\text{Mo}_2\{\mu-\text{MeLi}(\text{thf})\text{Me}\}(\mu-\text{Me})(\mu-\text{Ad}^{\text{Dipp2}})_2]$ .<sup>47,56</sup> The energy for the dissociation of  $4\cdot\text{thf}'$  to  $(\text{thf})\text{Li}-\text{H}$  and dihydride  $[\text{Mo}_2(\text{H})_2(\mu-\text{Ad}^{\text{Dipp2}})_2]$  given by our calculations is 27.9 kcal/mol, while the dissociation of two molecules of  $(\text{thf})\text{Li}-\text{H}$  from  $4\cdot\text{thf}$  is 55.1 kcal/mol. The NBO analysis discloses four orbitals that are responsible for the  $\sigma$  component, two  $\pi$  components, and one  $\delta$  component of the quadruple  $\text{Mo}-\text{Mo}$  bond (Figure 4a). In addition, we find that the  $dx^2-y^2$  orbitals, not involved in  $\text{Mo}-\text{Mo}$  bonding, form spd hybrids directed toward the hydrides<sup>47</sup> and combine with  $s(\text{H})$  orbitals to form the two  $\text{Mo}-\text{H}$  bonds (one of which is shown in Figure 4a).

The NBO approach results in limited participation of the lithium atomic orbitals in occupied MOs. However, this does not mean that its interactions with the hydrides and the molybdenum atoms are strictly ionic, since the calculated charge on Li is +0.67, indicative of a non-negligible covalent contribution. The reduced charge of the lithium “ion” is thus associated, in addition to  $\text{thf} \rightarrow \text{Li}$  donation, with two sets of donor–acceptor interactions: (i) donation from  $\sigma(\text{Mo}-\text{H})$  to Li and (ii) donation from the components of the  $\text{Mo}\equiv\text{Mo}$  bond to Li (Figure 4c).

From the energy point of view, there are two sets of dominant interactions (Figure 5a) that imply donations from the  $\sigma(\text{Mo}-\text{H})$  and  $\sigma(\text{Mo}'-\text{H})$  bonds to both  $s(\text{Li})$  and  $p_z(\text{Li})$  and from the  $\sigma$  component of the  $\text{Mo}\equiv\text{Mo}$  bond to the atomic orbitals of Li. In the first set, we find donation from  $\sigma(\text{Mo}-\text{H})$  to both  $s(\text{Li})$  and  $p_z(\text{Li})$ , which are responsible for 84% of the interaction energy. Among the second set of interactions, donation from  $\sigma(\text{Mo}-\text{Mo})$  to  $s(\text{Li})$  (Figure 4c) makes a significant contribution of 12%; smaller contributions come from the donations of  $\delta(\text{Mo}-\text{Mo})$  to  $p_x(\text{Li})$  and of  $\sigma(\text{Mo}-\text{Mo})$  to  $p_y(\text{Li})$ , while almost negligible contributions appear for  $\pi(\text{Mo}-\text{Mo})$  and for  $p_y$  and  $s(\text{Li})$ .

As a result of all of these donor–acceptor interactions from the  $\text{Mo}_2\text{H}_2$  moiety to the lithium ion, the distribution of the

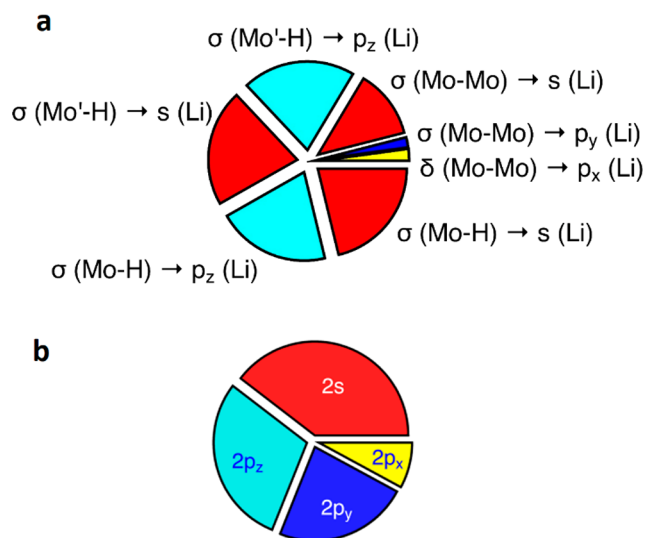


**Figure 5.** (a) Relative energy contributions of natural orbital donor–acceptor interactions between  $[\text{Mo}_2(\text{H})_2(\mu-\text{H})(\mu-\text{Ad}^{\text{Dipp2}})_2]^-$  and  $(\text{thf})\text{Li}^+$  fragments in  $4\cdot\text{thf}'$ . (b) Share of the Li valence electron density at each of its atomic orbitals, resulting from  $\sigma(\text{Mo}-\text{H}) \rightarrow \text{Li}$ ,  $\text{Mo}\equiv\text{Mo} \rightarrow \text{Li}$ , and  $\text{thf} \rightarrow \text{Li}$  donor–acceptor interactions.

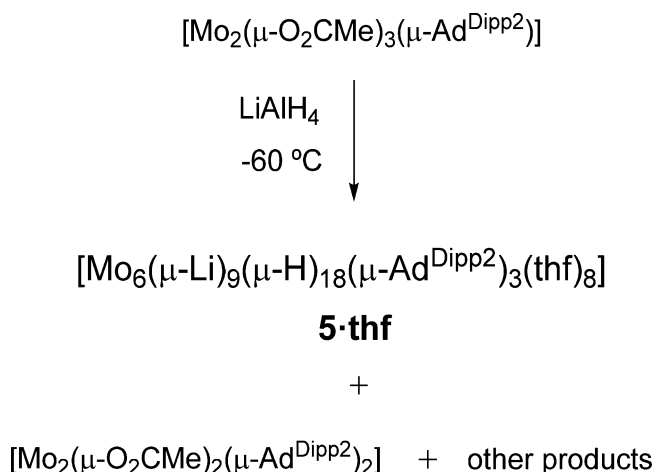
0.33 valence electron held by the Li atomic orbitals (Figure 5b) reflects the major role played by the  $2s$  and  $2p_z$  Li AOs as acceptors. The high population of the lithium  $p_y$  orbital compared to its minor acceptor role toward the  $\text{Mo}\equiv\text{Mo}$  group is undoubtedly due to the donation from its  $\text{thf}$  ligand. Finally, the lowest atomic orbital population in  $p_x$  results from the interesting donation from the  $\delta(\text{Mo}\equiv\text{Mo})$  bonding orbital (Figure 4c).

We can therefore conclude that the stability of the  $\text{Mo}-\text{H}-\text{Li}-\text{H}-\text{Mo}$  ring results mainly from the formation of two  $3c-2e$   $\text{Mo}-\text{H}-\text{Li}$  bonds, supplemented by  $\sigma$  coordination of the  $\text{Mo}\equiv\text{Mo}$  bond to the Li atom. The latter bonding component is consistent with a short distance between Li and the  $\text{Mo}\equiv\text{Mo}$  centroid of 2.77 Å ( $\text{Mo}-\text{Li} = 2.97$  Å), to be compared with a

covalent radii sum of 2.82 Å.<sup>55</sup> Although of lesser quantitative importance, the existence of non-negligible electron donation from the bonding  $\pi$  and  $\delta$ (Mo $\equiv$ Mo) orbitals is worth being stressed. The fact that the calculated dissociation energy of **4**·thf into (thf)Li–H and dihydride [Mo<sub>2</sub>(H)<sub>2</sub>( $\mu$ -Ad<sup>Dipp2</sup>)<sub>2</sub>] is 27.9 kcal/mol, smaller than the sum of NBO interaction energies shown in Figure 5a (98.7 kcal/mol), is explained by the high energy required to deform the (thf)Li–H group from linear in the free molecule to a highly bent (120°) geometry in **4**·thf as well as to modify the second coordination sphere of the Mo atoms to make room for the Li–thf moiety.

Having successfully built Mo<sub>2</sub>LiH<sub>2</sub> and Mo<sub>2</sub>Li<sub>2</sub>H<sub>4</sub> platforms based on Mo $\equiv$ Mo bonds coordinated to one and two H–Li(thf)–H units, respectively, our next goal was to explore the possibility of reaching a Mo<sub>2</sub>Li<sub>3</sub>H<sub>6</sub> organization in a purported [Mo<sub>2</sub>{HLi(thf)H}<sub>3</sub>( $\mu$ -Ad<sup>Dipp2</sup>)<sub>2</sub>] complex. To this end and taking into account the successful synthesis of complexes **3**·thf and **4**·thf by the procedure shown in Scheme 1c, we prepared tris(acetate) precursor [Mo<sub>2</sub>( $\mu$ -O<sub>2</sub>CMe)<sub>3</sub>( $\mu$ -Ad<sup>Dipp2</sup>)<sub>2</sub>] and performed its reaction with an excess of LiAlH<sub>4</sub>. Although the above Mo<sub>2</sub>Li<sub>3</sub>H<sub>6</sub> complex could not be observed, the transformation led to complex **5**·thf, identified as a polymetallic hydride cluster Mo<sub>6</sub>Li<sub>9</sub>H<sub>18</sub> (Scheme 2), that

**Scheme 2.** Formation of Hexamolybdenum Nonalithium Dodecaoctahydride Cluster **5**·thf



probably results from spontaneous trimerization of the targeted Mo<sub>2</sub>Li<sub>3</sub>H<sub>6</sub> monomer, with the loss of a molecule of tetrahydrofuran. The reaction was, however, complex and gave in addition compound [Mo<sub>2</sub>( $\mu$ -O<sub>2</sub>CMe)<sub>2</sub>( $\mu$ -Ad<sup>Dipp2</sup>)<sub>2</sub>] through an undisclosed reaction path. Like the bis(formate) analogue (Scheme 1c), the latter may react further with LiAlH<sub>4</sub>, justifying that isolated yields of **5**·thf are about 25%. Complex **5**·thf is very air-sensitive and decomposes instantly in the presence of oxygen and water, both in solution and in the solid state. Under strict anaerobic conditions, solutions in tetrahydrofuran or aromatic hydrocarbons remain unchanged at 25 °C for at least 24 h, although decomposition is fast above 50 °C.

The new supramolecular entity can be understood as a triangular array of [Mo<sub>2</sub>( $\mu$ -Ad<sup>Dipp2</sup>)<sub>2</sub>]<sup>3+</sup> components<sup>51,57,58</sup> connected by a [Li<sub>9</sub>H<sub>18</sub>]<sup>9–</sup> linker in a fairly robust manner. The Li-coordinated molecules of tetrahydrofuran were readily substituted by pyridine and 4-dimethylaminopyridine, giving complexes **5**·py and **5**·dmap without the alteration of the

molecular skeleton. Notwithstanding the foregoing, complex **5**·thf acted as an efficient source of LiH in the hydrolithiation of Ph<sub>2</sub>C(O) to give Ph<sub>2</sub>C(H)(OLi).<sup>20,22</sup> Somewhat unexpectedly, solutions of **5**·thf decomposed gradually upon stirring at room temperature under an atmosphere of H<sub>2</sub>, generating LiAd<sup>Dipp2</sup> as a byproduct. Dideuterium acted similarly and showed that H/D exchange took place, as attested to by NMR detection of HD along with H<sub>2</sub>. The H<sub>2</sub>-promoted cluster breakup was not investigated any further. Nevertheless, it seems plausible that H<sub>2</sub> may disrupt the cluster structure by displacing LiH molecules from the [Li<sub>9</sub>H<sub>18</sub>]<sup>9–</sup> linker, eliminating LiAd<sup>Dipp2</sup>. As an extension of these studies, various attempts were made to produce an alleged {Mo<sub>2</sub>(H)<sub>8</sub>[Li(thf)]<sub>4</sub>} complex (i.e., the hydride analogue of known methyl compound {Mo<sub>2</sub>(CH<sub>3</sub>)<sub>8</sub>[Li(OEt<sub>2</sub>)]<sub>4</sub>}).<sup>59</sup> As detailed in the SI, all essayed trials were unsuccessful.

The room-temperature <sup>1</sup>H NMR spectra of complexes **5**·L in C<sub>6</sub>D<sub>6</sub> or thf-*d*<sub>8</sub> solution show two septets and four doublets for the 12 isopropyl groups of the amidinate spectator ligands, in accordance with the proposed D<sub>3</sub> molecular symmetry (details in Supporting Information). The 18 H atoms that make up the [Li<sub>9</sub>H<sub>18</sub>]<sup>9–</sup> linker are expected to give rise to three resonances of equal relative intensity. Whereas for **5**·thf one of these signals seems to be hidden underneath other resonances, the three are clearly observed for complex **5**·py with chemical shifts of 2.04, 5.21, and 5.41 ppm. They appear as broad multiplets, but while the 2.04 peak becomes a singlet in the <sup>1</sup>H{<sup>7</sup>Li} NMR spectrum, the other two are converted to doublets with <sup>2</sup>J<sub>HH</sub> = 4 Hz. The <sup>7</sup>Li NMR spectrum contains three resonances centered at 5.4, 4.7, and 2.7 ppm, with relative intensities approaching roughly 6:2:1, once more in agreement with the proposed structure.

The molecular structure of complex **5**·thf was determined by X-ray crystallography (Figure 6) and computational studies. Since the calculated and experimental structures are very

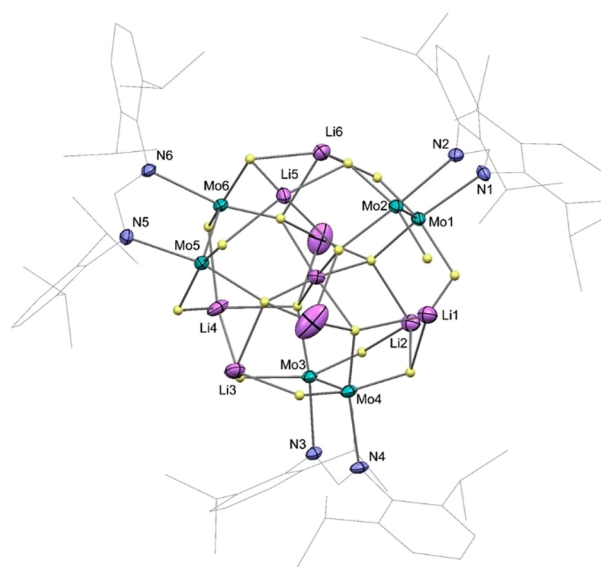


**Figure 6.** Solid-state structure of **5**·thf as determined by X-ray diffraction. Thermal ellipsoids are shown at 30%. Hydrogen atoms (except the hydride ligands) are omitted for clarity, as are thf molecules. Selected bond lengths (Å) and a bond angle (deg): Mo–Mo, 2.10 av.; Mo–Li9, 3.20 av.; Mo–N, 2.13 av.; Li9–Li7, 2.45(2); Li9–Li8, 2.50(2); Li7–Li9–Li8, 176.3(9).

similar (Table 1), all of the features that are discussed here based on the X-ray data also apply to the optimized geometry. The whole cluster is built up by successive concentric groups around a central  $\text{Li}_3$  unit (Figure 7, left) formed by Li7, Li9,

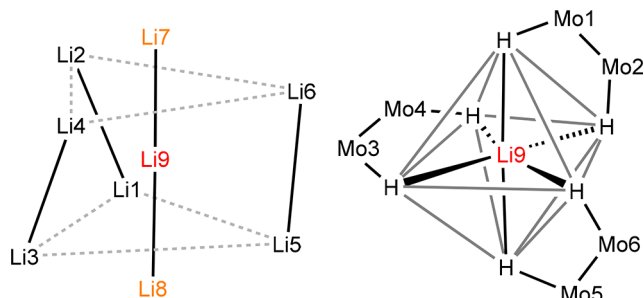


**Figure 7.**  $\text{Li}_9$  polyhedron present in the molecules of complex **5**-thf (left) and the distribution of H and Li atoms in the vicinity of central lithium atom Li9 (right).

and Li8 with a nearly linear arrangement ( $176(1)^\circ$ ) and distances of 2.50(2) and 2.45(2) Å, which are slightly shorter than twice the lithium covalent radius (2.56 Å).<sup>55</sup> We have been unable to locate a solid-state or gas-phase structure in which such a  $\text{Li}_3$  rod is present. The only  $\text{Li}_3$  group whose structure we are aware of appears in the crystal structure of  $\text{Li}_3[\text{IrD}_6]$ , with Li–Li distances of 2.58 and 2.76 Å and a Li–Li–Li angle of  $75.7^\circ$ .<sup>60</sup> The first concentric group around the central axis is composed of six  $\text{H}^{\text{ent}}$  atoms that provide a nearly octahedral coordination sphere to the central Li9 atom (Figure 7, right) and act as bridging atoms with the terminal atoms of the  $\text{Li}_3$  rod, with Li–H separations in the 1.70–2.20 Å interval. These hydrides are connected to the molybdenum atoms of the three  $\text{Mo}_2$  units that constitute the second concentric ring, with the shape of a slightly twisted trigonal prism and Mo–H distances in the range of 1.67–2.05 Å. The Mo–Mo bond length of 2.1020(7) Å is coherent with 4-fold bonding.<sup>51</sup>

Leaving aside the Li atoms, an ionic description of the cluster leaves us with three  $[\text{Mo}_2(\mu\text{-Ad}^{\text{Dipp2}})\text{H}_6]^{3-}$  blocks, in which each Mo atom bears two cis hydrides and one trans hydride relative to the N atoms of the  $\mu\text{-Ad}^{\text{Dipp2}}$  ligand. The latter have just been described as forming an  $\text{H}_6$  octahedron around the inner  $\text{Li}_3$  rod and being bonded to the three  $\text{Mo}_2$  units as well. The 12 cis hydrides can be described as distorted trigonal prisms, one with the trigonal faces roughly at the height of the external atoms of the central  $\text{Li}_3$  rod, or  $\text{H}_6^{\text{ext}}$  group, and the other with the trigonal faces very close to the central Li9 atom, or  $\text{H}_6^{\text{int}}$ . Finally, the six peripheral Li atoms form another trigonal prism (Figure 7, left) with one of the triangular faces (Li1, Li3, and Li5) rotated *ca.*  $13^\circ$  relative to the other (Li2, Li4, and Li6). Those Li atoms form three  $\text{Li}_2$  dumbbells with Li...Li distances of 2.83–2.90 Å and are supported by hydride bridges to neighboring Li and Mo atoms, with Li–H separations in the range of 1.74–2.29 Å (section 5 in the Supporting Information).

## CONCLUSIONS

We have demonstrated that a monomeric molecule of LiH can bind to the unsaturated molybdenum atom of  $[(\text{H})\text{Mo}\equiv\text{Mo}]$  entities by means of a  $3c-2e$  Mo–H→Li interaction combined with a  $\sigma\text{-Li-H}\rightarrow\text{Mo}$  bond.  $[\text{Mo}_2\{\mu\text{-HLi}(\text{thf})\text{H}\}_n]$  skeletons containing five-membered H–Mo≡Mo–H–Li rings have been constructed in this manner for  $n = 1$  and 2. When  $n$

$= 3$ , trimerization of the purported  $[\text{Mo}_2\{\mu\text{-HLi}(\text{thf})\text{H}\}_3(\mu\text{-Ad}^{\text{Dipp2}})]$  monomer occurs spontaneously, leading to a hydride-rich  $\text{Mo}_6\text{Li}_9\text{H}_{18}$  supramolecular organization that features an uncommon linear  $\text{Li}_3$  group around which are organized  $\text{Mo}_6$ ,  $\text{Li}_6$ , and two  $\text{H}_6$  polyhedra with shapes intermediate between an octahedron and compressed trigonal prisms.

## ASSOCIATED CONTENT

### Supporting Information

The Supporting Information is available free of charge at <https://pubs.acs.org/doi/10.1021/jacs.1c01602>.

Relevant experimental and calculated bonding parameters for **3**-thf, **4**-thf and **5**-thf; computational details; and atomic coordinates for the optimized geometries of the same compounds; synthesis and characterization of compounds (PDF)

Olex2 1.3 data (PDF)

## Accession Codes

CCDC 2059184–2059187 contain the supplementary crystallographic data for this paper. These data can be obtained free of charge via [www.ccdc.cam.ac.uk/data\\_request/cif](http://www.ccdc.cam.ac.uk/data_request/cif), or by emailing [data\\_request@ccdc.cam.ac.uk](mailto:data_request@ccdc.cam.ac.uk), or by contacting The Cambridge Crystallographic Data Centre, 12 Union Road, Cambridge CB2 1EZ, UK; fax: +44 1223 336033.

## AUTHOR INFORMATION

### Corresponding Authors

**Santiago Alvarez** – Department de Química Inorgànica i Orgànica, Secció de Química Inorgànica, and Institut de Química Teòrica i Computacional, Universitat de Barcelona, 08028 Barcelona, Spain; Email: [santiago.alvarez@qi.ub.es](mailto:santiago.alvarez@qi.ub.es)

**Ernesto Carmona** – Instituto de Investigaciones Químicas (IIQ), Departamento de Química Inorgànica and Centro de Innovación en Química Avanzada (ORFEO-CINQA), Consejo Superior de Investigaciones Científicas (CSIC), University of Sevilla, 41092 Sevilla, Spain; [orcid.org/0000-0003-2449-5848](https://orcid.org/0000-0003-2449-5848); Email: [guzman@us.es](mailto:guzman@us.es)

### Authors

**Marina Perez-Jimenez** – Instituto de Investigaciones Químicas (IIQ), Departamento de Química Inorgànica and Centro de Innovación en Química Avanzada (ORFEO-CINQA), Consejo Superior de Investigaciones Científicas (CSIC), University of Sevilla, 41092 Sevilla, Spain

**Natalia Curado** – Instituto de Investigaciones Químicas (IIQ), Departamento de Química Inorgànica and Centro de Innovación en Química Avanzada (ORFEO-CINQA), Consejo Superior de Investigaciones Científicas (CSIC), University of Sevilla, 41092 Sevilla, Spain

**Celia Maya** – Instituto de Investigaciones Químicas (IIQ), Departamento de Química Inorgànica and Centro de Innovación en Química Avanzada (ORFEO-CINQA), Consejo Superior de Investigaciones Científicas (CSIC), University of Sevilla, 41092 Sevilla, Spain

**Jesus Campos** – Instituto de Investigaciones Químicas (IIQ), Departamento de Química Inorgànica and Centro de Innovación en Química Avanzada (ORFEO-CINQA), Consejo Superior de Investigaciones Científicas (CSIC), University of Sevilla, 41092 Sevilla, Spain; [orcid.org/0000-0002-5155-1262](https://orcid.org/0000-0002-5155-1262)



Jesus Jover – Department de Química Inorgànica i Orgànica, Secció de Química Inorgànica, and Institut de Química Teòrica i Computacional, Universitat de Barcelona, 08028 Barcelona, Spain; [orcid.org/0000-0003-3383-4573](https://orcid.org/0000-0003-3383-4573)

Complete contact information is available at:  
<https://pubs.acs.org/10.1021/jacs.1c01602>

## Notes

The authors declare no competing financial interest.

## ACKNOWLEDGMENTS

This work has been supported by the Spanish Ministry of Economy and Competitiveness (PID2019-110856GA-I00 and PGC2018-093863-B-C21), the Spanish Structures of Excellence *María de Maeztu* program (grant MDM-2017-0767), and the Generalitat de Catalunya - AGAUR (grant 2017-SGR-1289). M.P.-J. thanks the Spanish Ministry of Education and Ministry of Science, Innovation and Universities for an FPU Ph.D. fellowship.

## DEDICATION

This paper is dedicated to the memory of our esteemed colleague and friend Professor Malcolm L. H. Green, in recognition of his monumental contributions to inorganic chemistry, organometallic chemistry, and catalysis.

## REFERENCES

- (1) Johnson, J. A. Populating the periodic table: Nucleosynthesis of the elements. *Science* **2019**, *363*, 474–478.
- (2) Güsten, R.; Wiesemeyer, H.; Neufeld, D.; Menten, K. M.; Graf, U. U.; Jacobs, K.; Klein, B.; Ricken, O.; Risacher, C.; Stutzki, J. Astrophysical detection of the helium hydride ion HeH. *Nature* **2019**, *568*, 357–359.
- (3) Aldridge, S.; Downs, T. Hydrides of the Main-Group Metals: New Variations on an Old Theme. *Chem. Rev.* **2001**, *101*, 3366 and references therein.
- (4) Kelly, M. T. In *Structure and Bonding* 141; Bocarsly, A., Mingos, D. M. P., Eds.; Springer: Berlin, 2011; pp 169–201.
- (5) Klusener, P. A. A.; Brandsma, L.; Verkruijsse, H. D.; Schleyer, P. v. R.; Friedl, T.; Pi, R. Superactive Alkali Metal Hydride Metalation Reagents: LiH, NaH, and KH. *Angew. Chem., Int. Ed. Engl.* **1986**, *25*, 465–466.
- (6) Bickelhaupt, F. M.; Solà, M.; Fonseca Guerra, C. Highly polar bonds and the meaning of covalency and ionicity-structure and bonding of alkali metal hydride oligomers. *Faraday Discuss.* **2007**, *135*, 451–468.
- (7) Bellini, M.; De Natale, P.; Inguscio, M.; Varberg, T. D.; Brown, J. M. Precise experimental test of models for the breakdown of the Born-Oppenheimer separation: The rotational spectra of isotopic variants of lithium hydride. *Phys. Rev. A: At., Mol., Opt. Phys.* **1995**, *52*, 1954–1960.
- (8) Maitland, B.; Wiesinger, M.; Langer, J.; Ballmann, G.; Pahl, J.; Elsen, H.; Färber, C.; Harder, S. A Simple Route to Calcium and Strontium Hydride Clusters. *Angew. Chem., Int. Ed.* **2017**, *56*, 11880–11884.
- (9) Rauch, M.; Ruccolo, S.; Parkin, G. Synthesis, Structure, and Reactivity of a Terminal Magnesium Hydride Compound with a Carbatriene Motif, [TismPriBenz]MgH: A Multifunctional Catalyst for Hydrosilylation and Hydroboration. *J. Am. Chem. Soc.* **2017**, *139*, 13264–13267.
- (10) Arrowsmith, M.; Hill, M. S.; Kociok-Köhn, G.; MacDougall, D. J.; Mahon, M. F. Beryllium-Induced C–N Bond Activation and Ring Opening of an N-Heterocyclic Carbene. *Angew. Chem., Int. Ed.* **2012**, *51*, 2098–2100.
- (11) Bonyhady, S. J.; Jones, C.; Nembenna, S.; Stasch, A.; Edwards, A. J.; McIntyre, G. J.  $\beta$ -Diketiminato-Stabilized Magnesium(I) Dimers and Magnesium(II) Hydride Complexes: Synthesis, Characterization, Adduct Formation, and Reactivity Studies. *Chem. - Eur. J.* **2010**, *16*, 938–955.
- (12) Bonyhady, S.; Green, S.; Jones, C.; Nembenna, S.; Stasch, A. A dimeric magnesium(I) compound as a facile two-centre/two-electron reductant. *Angew. Chem., Int. Ed.* **2009**, *48*, 2973–2977.
- (13) Green, S.; Jones, C.; Stasch, A. Stable Adducts of a Dimeric Magnesium(I) Compound. *Angew. Chem., Int. Ed.* **2008**, *47*, 9079–9083.
- (14) Arrowsmith, M.; Hill, M. S.; Hadlington, H.; Kociok-Köhn, G.; Weetman, C. Magnesium-Catalyzed Hydroboration of Pyridines. *Organometallics* **2011**, *30*, 5556–5559.
- (15) Spielmann, J.; Harder, S. Hydrocarbon-Soluble Calcium Hydride: A “Worker-Bee” in Calcium Chemistry. *Chem. - Eur. J.* **2007**, *13*, 8928–8938.
- (16) Schuhknecht, D.; Spaniol, T. P.; Maron, L.; Okuda, J. Regioselective Hydrosilylation of Olefins Catalyzed by a Molecular Calcium Hydride Cation. *Angew. Chem., Int. Ed.* **2020**, *59*, 310–314.
- (17) Schnitzler, S.; Spaniol, T. P.; Okuda, J. Reactivity of a Molecular Magnesium Hydride Featuring a Terminal Magnesium–Hydrogen Bond. *Inorg. Chem.* **2016**, *55*, 12997–13006.
- (18) Schnitzler, S.; Spaniol, T. P.; Maron, L.; Okuda, J. Formation and Reactivity of a Molecular Magnesium Hydride with a Terminal Mg–H Bond. *Chem. - Eur. J.* **2015**, *21*, 11330–11334.
- (19) Arrowsmith, M.; Hill, M.; MacDougall, D.; Mahon, M. A Hydride-Rich Magnesium Cluster. *Angew. Chem., Int. Ed.* **2009**, *48*, 4013–4016.
- (20) Stasch, A. A Hydrocarbon-Soluble Lithium Hydride Complex. *Angew. Chem., Int. Ed.* **2012**, *51*, 1930–1933.
- (21) Campbell, R.; Cannon, D.; García-Alvarez, P.; Kennedy, A. R.; Mulvey, R. E.; Robertson, S. D.; Saßmannshausen, J.; Tuttle, T. Main Group Multiple C–H/N–H Bond Activation of a Diamine and Isolation of A Molecular Dilithium Zincate Hydride: Experimental and DFT Evidence for Alkali Metal–Zinc Synergistic Effects. *J. Am. Chem. Soc.* **2011**, *133*, 13706–13717.
- (22) Robertson, S. D.; Kennedy, A. R.; Liggat, J. J.; Mulvey, R. E. Facile synthesis of a genuinely alkane-soluble but isolable lithium hydride transfer reagent. *Chem. Commun.* **2015**, *51*, 5452–5455.
- (23) Haywood, J.; Wheatley, A. E. H. Hydride encapsulation by molecular alkali-metal clusters. *Dalton Trans.* **2008**, 3378–3397.
- (24) Hoffmann, D.; Kottke, T.; Lagow, R. J.; Thomas, R. D. X-Ray Structural Analysis of a Novel Lithium Hydride/Lithium *tert*-Butoxide Superaggregate: Li<sub>33</sub>H<sub>17</sub>(OtBu)<sub>16</sub>. *Angew. Chem., Int. Ed.* **1998**, *37*, 1537–1539.
- (25) Veith, M.; König, P.; Rammo, A.; Huch, V. Cubane-Like Li<sub>4</sub>H<sub>4</sub> and Li<sub>3</sub>H<sub>3</sub>Li(OH): Stabilized in Molecular Adducts with Alanes. *Angew. Chem., Int. Ed.* **2005**, *44*, 5968–5971.
- (26) Fischer, K.; Jonas, K.; Misbach, P.; Stabba, R.; Wilke, G. The “Nickel Effect”. *Angew. Chem., Int. Ed. Engl.* **1973**, *12*, 943–953.
- (27) Goddard, R.; Krüger, C.; Pörschke, K. R.; Wilke, G. Elektronendichte-verteilungen in metallorganischen verbindungen. Wechselnde struktur- und bindungsverhältnisse in dimeren metallorganischen nickel-hydriden mit ionenpaar-beziehungen zu den hauptgruppen-metallen natrium und lithium. *J. Organomet. Chem.* **1986**, *308*, 85–103.
- (28) Pörschke, K. R.; Wilke, G. Zur Lewisacidität von Nickel(0): VII. Alkalimetall- $\mu_3$ -hydrido-tetrakis(ethen)dinickolat(0)-Komplexe: (pmdta) Li( $\mu_3$ -H)Ni<sub>2</sub>(C<sub>2</sub>H<sub>4</sub>)<sub>4</sub> und (pmdta)Na( $\mu_3$ -H)Ni<sub>2</sub>(C<sub>2</sub>H<sub>4</sub>)<sub>4</sub>. *J. Organomet. Chem.* **1988**, *349*, 257–261.
- (29) Gilbert, T. M.; Bergman, R. G. NMR spectra of (C5(CH3)5)IrH2SiMe3Li(pmdeta) and (C5(CH3)5)IrH3Li(pmdeta): the first direct observation of resolved lithium-7-proton coupling. *J. Am. Chem. Soc.* **1985**, *107*, 6391–6393.
- (30) Heine, A.; Stalke, D. Structures of Two Highly Reactive Intermediates upon LiAlH<sub>4</sub> Reduction in the Solid State and in Solution: [(Me<sub>3</sub>Si)<sub>2</sub>NAIH<sub>3</sub>Li·2Et<sub>2</sub>O]<sub>2</sub> and [(Me<sub>3</sub>Si)<sub>2</sub>N]<sub>2</sub>AlH<sub>2</sub>Li·2Et<sub>2</sub>O. *Angew. Chem., Int. Ed. Engl.* **1992**, *31*, 854–855.
- (31) Liu, H.-J.; Ziegler, M. S.; Tilley, T. D. Ring-opening and double-metallation reactions of the N-Heterocyclic carbene ligand in



Cp\*(IXy)Ru (IXy = 1,3-bis(2,6-dimethylphenyl)imidazol-2-ylidene) complexes. Access to an anionic fischer-type carbene complex of ruthenium. *Polyhedron* **2014**, *84*, 203–208.

(32) Berry, A.; Green, M. H. L.; Bandy, J. A.; Prout, K. J. *Chem. Soc., Transition metal–hydrogen–alkali metal bonds: synthesis and crystal structures of* [K(18-crown-6)][W(PMe<sub>3</sub>)<sub>3</sub>H<sub>5</sub>], [Na(15-crown-5)][W(PMe<sub>3</sub>)<sub>3</sub>H<sub>5</sub>] and [{W(PMe<sub>3</sub>)<sub>3</sub>H<sub>5</sub>Li}<sub>4</sub>] and related studies. *J. Chem. Soc., Dalton Trans.* **1991**, 2185–2206.

(33) Bohra, R.; Hitchcock, P. B.; Lappert, M. F.; Au-Yeung, S. C. F.; Leung, W.-P. Group 6 metallocene(IV)–main group metal complexes: synthesis and structures of a Mo–B–Li compound and of [W(η-C<sub>5</sub>H<sub>5</sub>)<sub>2</sub>H{SnCl<sub>2</sub>CH(SiMe<sub>3</sub>)<sub>2</sub>}]. *J. Chem. Soc., Dalton Trans.* **1995**, 2999–3005.

(34) Plois, M.; Wiegand, T.; Wolf, R. Novel Ruthenium(II) Aluminate Anions: Building Blocks of Unique Cage Structures. *Organometallics* **2012**, *31*, 8469–8477.

(35) Schmidt, J. A. R.; Arnold, J. Alkyl and Alkylidene Tantalum–Lithium Complexes Supported by an Anionic Triazacyclononane Ligand. *Organometallics* **2002**, *21*, 3426–3433.

(36) Riddlestone, I. M.; Abdalla, J. A. B.; Aldridge, S. Coordination and Activation of E–H Bonds (E = B, Al, Ga) at Transition Metal Centers. *Adv. Organomet. Chem.* **2015**, *63*, 1–38.

(37) Abdalla, J. A. B.; Riddlestone, I. M.; Tirfoin, R.; Phillips, N.; Bates, J. I.; Aldridge, S. Al–H σ-bond coordination: expanded ring carbene adducts of AlH<sub>3</sub> as neutral bi- and tri-functional donor ligands. *Chem. Commun.* **2013**, 49, 5547–5549.

(38) Turner, J.; Abdalla, J. A. B.; Bates, J. I.; Tirfoin, R.; Kelly, M. J.; Phillips, N.; Aldridge, S. Formation of sub-valent carbenoid ligands by metal-mediated dehydrogenation chemistry: coordination and activation of H<sub>2</sub>Ga{(NDippCMe)<sub>2</sub>CH}. *Chem. Sci.* **2013**, *4*, 4245–4250.

(39) Riddlestone, I. M.; Edmonds, S.; Kaufman, P. A.; Urbano, J.; Bates, J. I.; Kelly, M. J.; Thompson, A. L.; Taylor, R.; Aldridge, S. σ-Alane Complexes of Chromium, Tungsten, and Manganese. *J. Am. Chem. Soc.* **2012**, *134*, 2551–2554.

(40) Ekkert, O.; White, A. J. P.; Crimmin, M. R. Trajectory of Approach of a Zinc–Hydrogen Bond to Transition Metals. *Angew. Chem., Int. Ed.* **2016**, *55*, 16031–16034.

(41) Ekkert, O.; White, A. J. P.; Tomsb, H.; Crimmin, M. R. Addition of aluminium, zinc and magnesium hydrides to rhodium(III). *Chem. Sci.* **2015**, *6*, 5617–5622.

(42) Garçon, M.; Bakewell, C.; Sackman, G.; White, A. J. P.; Cooper, R. I.; Edwards, A. J.; Crimmin, M. R. A hexagonal planar transition-metal complex. *Nature* **2019**, *574*, 390–393.

(43) Riddlestone, I. M.; Rajabi, N. A.; Lowe, J. P.; Mahon, M. F.; Macgregor, S. A.; Whittlesey, M. K. Activation of H<sub>2</sub> over the Ru–Zn Bond in the Transition Metal–Lewis Acid Heterobimetallic Species [Ru(IPr)<sub>2</sub>(CO)ZnEt]. *J. Am. Chem. Soc.* **2016**, *138*, 11081–11084.

(44) Butler, M. J.; Crimmin, M. R. Magnesium, zinc, aluminium and gallium hydride complexes of the transition metals. *Chem. Commun.* **2017**, 53, 1348–1365.

(45) Perez-Jimenez, M.; Curado, N.; Maya, C.; Campos, J.; Ruiz, E.; Álvarez, S.; Carmona, E. Experimental and Computational Studies on Quadruply Bonded Dimolybdenum Complexes with Terminal and Bridging Hydride Ligands. *Chem. - Eur. J.* **2021**, DOI: 10.1002/chem.202004948.

(46) Green, J.; Green, M. L. H.; Parkin, G. The occurrence and representation of three-centre two-electron bonds in covalent inorganic compounds. *Chem. Commun.* **2012**, 48, 11481–11503.

(47) Curado, N.; Carrasco, M.; Maya, C.; Peloso, R.; Rodríguez, A.; Ruiz, E.; Álvarez, S.; Carmona, E. An Unsaturated Four-Coordinate Dimethyl Dimolybdenum Complex with a Molybdenum–Molybdenum Quadruple Bond. *Chem. - Eur. J.* **2017**, *23*, 194–205.

(48) Mendoza, L.; Curado, N.; Carrasco, M.; Álvarez, E.; Peloso, R.; Rodríguez, A.; Carmona, E. Synthesis and structure of mixed carboxylate-aminopyridinate and -amidinate complexes of dimolybdenum and tungsten. *Inorg. Chim. Acta* **2015**, *424*, 120–128.

(49) Del Bene, J. E.; Alkorta, I.; Elguero, J. Ab Initio Study of Ternary Complexes A···NCH···C with A, C = HCN, HF, HCl, ClF,

and LiH: Energetics and Spin–Spin Coupling Constants across Intermolecular Bonds. *J. Phys. Chem. A* **2010**, *114*, 8463–8473.

(50) The Cambridge Structural Database; Groom, C. R.; Bruno, I. J.; Lightfoot, M. P.; Ward, S. C. The Cambridge Structural Database. *Acta Crystallogr.* **2016**, *B72*, 171–179.

(51) Cotton, F. A.; Murillo, L. A.; Walton, R. A. *Multiple Bonds Between Metal Atoms*; Springer: New York, 2005.

(52) Liddle, S. T. *Molecular Metal–Metal Bonds: Compounds, Synthesis, Properties*; Wiley-VCH, 2015.

(53) Krogman, J. P.; Thomas, C. M. Metal-metal multiple bonding in C<sub>3</sub>-symmetric bimetallic complexes of the first row transition metals. *Chem. Commun.* **2014**, 50, 5115–5127.

(54) Bau, R.; Drabnis, M. H. Structures of transition metal hydrides determined by neutron diffraction. *Inorg. Chim. Acta* **1997**, *259*, 27–50.

(55) Cordero, B.; Gómez, V.; Platero-Prats, A. E.; Revés, M.; Echeverría, J.; Cremades, E.; Barragán, F.; Álvarez, S. Covalent radii revisited. *Dalton Trans.* **2008**, 2832–2838.

(56) Curado, N.; Carrasco, M.; Álvarez, E.; Maya, C.; Peloso, R.; Rodríguez, A.; Lopez-Serrano, J.; Carmona, E. Lithium Di- and Trimethyl Dimolybdenum(II) Complexes with Mo–Mo Quadruple Bonds and Bridging Methyl Groups. *J. Am. Chem. Soc.* **2015**, *137*, 12378–12387.

(57) Cotton, F. A.; Liu, C. Y.; Murillo, C. A.; Wang, X. Dimolybdenum-Containing Molecular Triangles and Squares with Diamidate Linkers: Structural Diversity and Complexity. *Inorg. Chem.* **2006**, *45*, 2619–2626.

(58) Li, J.-R.; Yakovenko, A. A.; Lu, W.; Timmons, D. J.; Zhuang, W.; Yuan, D.; Zhou, H.-C. Ligand Bridging-Angle-Driven Assembly of Molecular Architectures Based on Quadruply Bonded Mo–Mo Dimers. *J. Am. Chem. Soc.* **2010**, *132*, 17599–17610.

(59) Cotton, F. A.; Troup, J. M.; Webb, T. R.; Williamson, D. H.; Wilkinson, G. Preparation, chemistry, and structure of the lithium salt of the octamethyldimolybdate (II) ion. *J. Am. Chem. Soc.* **1974**, *96*, 3824–3828.

(60) Gehlen, W.; Bronger, M.; Auffermann, G. Na<sub>3</sub>RhH<sub>6</sub>, Na<sub>3</sub>IrH<sub>6</sub> und Li<sub>3</sub>IrH<sub>6</sub>, neue komplexe Hydride mit isolierten [RhH<sub>6</sub>]<sup>3-</sup> und [IrH<sub>6</sub>]<sup>3-</sup> Oktaedern. *J. Alloys Compd.* **1991**, *176*, 255–262.